IOPscience iopscience.iop.org

Home Search Collections Journals About Contact us My IOPscience

Instability of the collinear phase in a two-dimensional ferromagnet in a strong in-plane magnetic field

This article has been downloaded from IOPscience. Please scroll down to see the full text article.

2009 J. Phys.: Condens. Matter 21 216009

(http://iopscience.iop.org/0953-8984/21/21/216009)

View the table of contents for this issue, or go to the journal homepage for more

Download details:
IP Address: 129.252.86.83
The article was downloaded on 29/05/2010 at 19:55

Please note that terms and conditions apply.

J. Phys.: Condens. Matter **21** (2009) 216009 (10pp) doi:10.1088/0953-8984/21/21/216009

# Instability of the collinear phase in a two-dimensional ferromagnet in a strong in-plane magnetic field

**A V Syromyatnikov**

Petersburg Nuclear Physics Institute, Gatchina, St Petersburg 188300, Russia

E-mail: syromyat@thd.pnpi.spb.ru

Received 21 January 2009, in final form 9 April 2009
Published 1 May 2009
Online at stacks.iop.org/JPhysCM/21/216009

**Abstract**

It is well-known that in a thin ferromagnetic film with a net magnetization perpendicular to the film the collinear arrangement of spins is unstable in an in-plane field $H$ smaller than its saturation value $H_c$. The existence of a stripe phase was proposed with elongated domains of alternating direction of the magnetization component perpendicular to the film. We consider in the present paper the strong-field regime $H < H_c$ and discuss the minimal microscopic model describing this phenomenon, a two-dimensional Heisenberg ferromagnet with strong easy-axis anisotropy and dipolar forces. The noncollinear (stripe) phase is discussed using the technique of Bose–Einstein condensation of magnons. Some previously unknown results are observed concerning the stripe phase. Evolution of the spin arrangement in the noncollinear phase is established upon field rotation within the plane. We find a rapid decrease of the period of the stripe structure as the field decreases. We demonstrate that spin components perpendicular to the film form a sinusoid in the noncollinear phase at $H \approx H_c$ that transforms to a step-like profile with decreasing field so that the domain wall density decreases from unity to a value much smaller than unity. The spin-wave spectrum in the noncollinear phase is discussed.

(Some figures in this article are in colour only in the electronic version)

## 1. Introduction

Numerous fascinating magnetic properties of ultrathin films and (quasi-) two-dimensional (2D) magnetic materials are attracting much attention now that it is also stimulated by the technological significance of such materials [1, 2]. One of the most intriguing experimental findings was the discovery of spin reorientation transition (SRT) in thin ferromagnetic films [3]. Recent experimental and theoretical investigations have shown that SRT can be induced by the temperature, the film thickness or by an applied magnetic field. In most cases the rotation occurs during SRT from the perpendicular to an in-plane direction (or vice versa) of film magnetization. In many materials with the net magnetization perpendicular to the film this reorientation is accompanied by stripe phases with elongated domains of alternating magnetization direction which are separated by domain walls with a finite width. Such transition was obtained first in [4] in Co/Au(111) films. The reader is referred to the comprehensive reviews of numerous recent experimental and theoretical works in this field [1, 2]. It is well established now that the origin of SRT and the stripe phases is in the subtle interplay between the short-range exchange, anisotropy and long-range dipolar interactions between spins [1, 2]. Then, a realistic theoretical model of low-dimensional magnetic systems must include these three kinds of interaction so that the Hamiltonian has the form of the minimal microscopic model showing SRT and the stripe phase

$$\mathcal{H} = -\tfrac{1}{2}\sum_{l\neq m}(J_{lm}\delta_{\rho\beta} + Q_{lm}^{\rho\beta})S_l^\rho S_m^\beta - A\sum_l (S_l^y)^2 - H\sum_l S_l^z, \quad (1)$$

$$Q_{lm}^{\rho\beta} = (g\mu)^2 \frac{3R_{lm}^\rho R_{lm}^\beta - \delta_{\rho\beta}R_{lm}^2}{R_{lm}^5}, \quad (2)$$

where we direct the $y$-axis perpendicular to the lattice as shown in figure 1 and the last term describes the Zeeman energy in the in-plane field discussed below.

 © 2009 IOP Publishing Ltd Printed in the UK

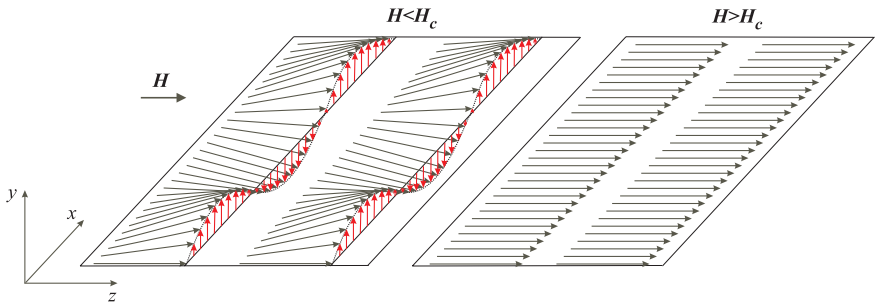


**Figure 1.** Two phases of the model (1) in a strong magnetic field $H$: those with collinear and noncollinear spin orderings at $H > H_c$ and $H < H_c$, respectively. Off-plane spin components are shown in red in the stripe phase (i.e. at $H < H_c$). It is obtained in the present paper that these components form a sinusoid at $H \approx H_c$ that transforms to a step-like profile with decreasing field, as shown in figure 4. The period of the stripe pattern increases as the field decreases, as presented in figure 5.

It is demonstrated in [5] that at $H = 0$ and $T = 0$ the stripe arrangement of spins in the model (1) has a slightly smaller energy than any collinear arrangement if $2A > \alpha\omega_0$ (i.e. if the easy direction is normal to the film), where

$$\alpha = \frac{3v_0}{8\pi}\sum_i \frac{1}{R_i^3} \tag{3}$$

is a constant that is approximately equal to 1.078 for the simple square lattice,

$$\omega_0 = 4\pi(g\mu)^2 \tag{4}$$

is the characteristic dipolar energy and we set the lattice spacing to be equal to unity. Meanwhile it was found in [5] that the period of the stripe structure rises rapidly as the value of the anisotropy increases so that the domain width is macroscopically large (i.e. larger than the $10^8$ lattice spacing) for $2A > 1.4\alpha\omega_0$. It is implied hereafter that $J \gg \omega_0$, as it usually is. We assume in the present paper that $2A > 1.4\alpha\omega_0$ and consider a macroscopically large unidomain sample with all spins directed perpendicular to the film at $H = 0$. It is also assumed below that $J \gg A$.

The existence of a stripe phase in this case was pointed out a long time ago [6] in an interval of an in-plane magnetic field $H_c' < H < H_c$, where $H_c$ is the saturation field and

$$H_c' = H_c - \tfrac{3}{2}Dk_{c0}^2. \tag{5}$$

The experimental evidence for the in-plane field-induced collinear phase instability was reported recently in Ni(001) ultrathin films at room temperature [7]. It was pointed out in [6] that the spin-wave spectrum calculated in the linear spin-wave approximation assuming a collinear spin arrangement is unstable when $H_c' < H < H_c$. Importantly, the instability occurs not at zero momentum but at a finite incommensurate one $\mathbf{k}_{c0}$, the direction of which is not fixed in the linear spin-wave approximation and the value of which is given by

$$k_{c0} = \frac{S\omega_0}{4D}, \tag{6}$$

where $D$ is the spin-wave stiffness that is equal, in particular, to $SJ$ for a simple square lattice with exchange coupling constant $J$ between neighboring spins. As a result it was proposed that the model (1) shows three phases in a nonzero in-plane field—a collinear one at $H > H_c$, a collinear canted phase at $H < H_c'$, and a noncollinear one appearing at $H_c' < H < H_c$. The properties of the noncollinear phase have not been clarified yet. It was proposed in [6] that there should be a domain pattern at $H_c' < H < H_c$ with a period equal to $2\pi/k_{c0}$ formed by spins components perpendicular to the film, similar to that discussed in [5] for $H = 0$.

It should be pointed out, however, that the stability of the spin-wave spectrum is not a criterion for the corresponding state to be the ground state. Then it is not clear at which field $H_c'$ the transition takes place from the stripe phase to a canted collinear one. It is not clear either whether such a transition happens at all, because the stripe phase has lower energy at $H = 0$, as shown in [5].

Despite great recent interest in exotic noncollinear phases, that of the model (1) in a strong-field regime has not been discussed thoroughly yet. The aim of the present paper is to try and fill this gap. We discuss first $1/S$ corrections to the spectrum in the collinear phase at $H > H_c$ and show that they fix the direction of $\mathbf{k}_{c0}$ at which the spectrum instability occurs and the absolute value of which is given by equation (6). We find the dependence of the $\mathbf{k}_{c0}$ direction on the field direction within the plane.

The noncollinear phase is discussed below using the technique of the Bose–Einstein condensation of magnons suggested in [8]. The transition to the stripe phase at $H = H_c$ corresponds within this technique to a 'condensation' of magnons at states characterized by a momentum $\mathbf{k}_c \parallel \mathbf{k}_{c0}$ and its harmonics (i.e. $n\mathbf{k}_c$, where $n$ is an integer). It is the unusual result of the present analysis that the vector $\mathbf{k}_c$ varies with the field (remaining parallel to $\mathbf{k}_{c0}$) so that $k_c = k_{c0}$ at $H = H_c$ and $k_c < k_{c0}$ at $H < H_c$. This unusual behavior is related to condensation of magnons at states characterized by harmonics of $\mathbf{k}_c$. Remember that the condensation in antiferromagnetic [8] and ferromagnetic [9] systems takes place at antiferromagnetic and zero (commensurate) vectors, respectively, which do not depend on the magnetic field. Thus, we find that the period of the stripe structure given by $2\pi/k_c$ rises very fast as the field decreases.

We demonstrate that the energy of the stripe phase is lower than the energy of any collinear spin arrangement at $H < H_c$ but the difference between these energies decreases as the field reduces.

We find values of spin components perpendicular to the film forming the domain pattern. It is shown that spin components perpendicular to the film form a sinusoid in the noncollinear phase at $H \approx H_c$ that transforms to a step-like profile when the field decreases so that the domain wall density decreases from unity to a value much smaller than unity.

We also discuss below the spin-wave spectrum in the noncollinear phase.

The rest of the paper is organized as follows. We discuss the Hamiltonian transformation and technique in section 2. The magnon spectrum is discussed in the linear spin-wave approximation in section 3. First $1/S$ corrections to the spectrum at $H > H_c$ are discussed in section 4. Properties of the noncollinear phase are considered in section 5. Section 6 contains our conclusion. One appendix is added with some details of the calculations.

## 2. Hamiltonian transformation and technique

It is implied below that the in-plane magnetic field is directed arbitrarily relative to the lattice. Taking the Fourier transformation we have from equation (1)

$$\mathcal{H} = -\tfrac{1}{2}\sum_{\mathbf{k}}(J_{\mathbf{k}}\delta_{\rho\beta} + Q^{\rho\beta}_{\mathbf{k}})S^{\rho}_{\mathbf{k}}S^{\beta}_{-\mathbf{k}} - A\sum_{\mathbf{k}} S^{y}_{\mathbf{k}}S^{y}_{-\mathbf{k}} - H\sqrt{\mathfrak{N}}S^{z}_{\mathbf{0}}, \tag{7}$$

where $J_{\mathbf{k}} = \sum_l J_{lm}\exp(\mathrm{i}\mathbf{k}\mathrm{R}_{lm})$, $Q^{\rho\beta}_{\mathbf{k}} = \sum_l Q^{\rho\beta}_{lm}\exp(\mathrm{i}\mathbf{k}\mathbf{R}_{lm})$ and $\mathfrak{N}$ is the number of spins in the lattice. The dipolar tensor $Q^{\rho\beta}_{\mathbf{k}}$ possesses well-known properties [10, 1] at $k \ll 1$, which are independent of the lattice type and the orientation of the $x$- and $z$-axes relative to the lattice,

$$Q^{\rho\beta}_{\mathbf{k}} = \omega_0\left(\frac{\alpha}{3}\delta_{\rho\beta} - \frac{k}{2}\frac{k_\rho k_\beta}{k^2}\right), \qquad \text{where } \rho, \beta = x, z, \tag{8}$$

$$Q^{y\beta}_{\mathbf{k}} = \omega_0\left(-\frac{2}{3}\alpha + \frac{k}{2}\right)\delta_{y\beta}, \qquad \text{where } \beta = x, y, z, \tag{9}$$

where $\alpha$ and $\omega_0$ are given by equations (3) and (4), respectively. It is seen from equations (1), (8) and (9) that dipolar forces lead to easy-plane anisotropy in the energy of the classical 2D FM with $y$ to be a hard axis [10]. Quantum and thermal fluctuations also lead to an in-plain anisotropy (the order-by-disorder effect) [11–13].

In the present paper we use the well-known representation of spin components via the Bose operators $a$ and $a^\dagger$ [14]:

$$S^{-}_i \approx \sqrt{2S}a^\dagger_i\left(1 - \frac{a^\dagger_i a_i}{4S}\right), \qquad S^{\dagger}_i \approx \sqrt{2S}\left(1 - \frac{a^\dagger_i a_i}{4S}\right)a_i, \qquad S^z_i = S - a^\dagger_i a_i \tag{10}$$

which can be obtained from the Holstein–Primakoff transformation [15] by expanding the square roots up to the first terms.

To perform the calculations it is convenient to introduce the following retarded Green's functions: $G(\omega, \mathbf{k}) = \langle a_{\mathbf{k}}, a^\dagger_{\mathbf{k}}\rangle_\omega$, $F(\omega, \mathbf{k}) = \langle a_{\mathbf{k}}, a_{-\mathbf{k}}\rangle_\omega$, $\bar{G}(\omega, \mathbf{k}) = \langle a^\dagger_{-\mathbf{k}}, a_{-\mathbf{k}}\rangle_\omega = G^*(-\omega, -\mathbf{k})$ and $F^\dagger(\omega, \mathbf{k}) = \langle a^\dagger_{-\mathbf{k}}, a^\dagger_{\mathbf{k}}\rangle_\omega = F^*(-\omega, -\mathbf{k})$. We have the following set of Dyson equations:

$$\begin{aligned} G(\omega, \mathbf{k}) &= G^{(0)}(\omega, \mathbf{k}) + G^{(0)}(\omega, \mathbf{k})\bar{\Sigma}(\omega, \mathbf{k})G(\omega, \mathbf{k}) \\ &\quad + G^{(0)}(\omega, \mathbf{k})[B_{\mathbf{k}} + \Pi(\omega, \mathbf{k})]F^\dagger(\omega, \mathbf{k}), \\ F^\dagger(\omega, \mathbf{k}) &= \bar{G}^{(0)}(\omega, \mathbf{k})\Sigma(\omega, \mathbf{k})F^\dagger(\omega, \mathbf{k}) \\ &\quad + \bar{G}^{(0)}(\omega, \mathbf{k})[B_{\mathbf{k}} + \Pi^\dagger(\omega, \mathbf{k})]G(\omega, \mathbf{k}), \end{aligned} \tag{11}$$

where $G^{(0)}(\omega, \mathbf{k}) = (\omega - E_{\mathbf{k}} + \mathrm{i}\delta)^{-1}$ is the bare Green's function, $\Sigma(\omega, \mathbf{k}) = \bar{\Sigma}(-\omega, -\mathbf{k})^*$, $\Pi(\omega, \mathbf{k}) = \Pi^\dagger(-\omega, -\mathbf{k})^*$ are the self-energy parts and $E_{\mathbf{k}}$ and $B_{\mathbf{k}}$ are coefficients in the bilinear part of the Hamiltonian

$$\mathcal{H}_2 = \sum_{\mathbf{k}}\left[E_{\mathbf{k}}a^\dagger_{\mathbf{k}}a_{\mathbf{k}} + \frac{B_{\mathbf{k}}}{2}(a_{\mathbf{k}}a_{-\mathbf{k}} + a^\dagger_{\mathbf{k}}a^\dagger_{-\mathbf{k}})\right] \tag{12}$$

which are presented below. Solving equations (11) one obtains

$$\begin{aligned} G(\omega, \mathbf{k}) &= \frac{\omega + E_{\mathbf{k}} + \Sigma(\omega, \mathbf{k})}{\mathcal{D}(\omega, \mathbf{k})}, \\ F(\omega, \mathbf{k}) &= -\frac{B_{\mathbf{k}} + \Pi(\omega, \mathbf{k})}{\mathcal{D}(\omega, \mathbf{k})}, \end{aligned} \tag{13}$$

where

$$\mathcal{D}(\omega, \mathbf{k}) = (\omega + \mathrm{i}\delta)^2 - \epsilon^2_{\mathbf{k}} - \Omega(\omega, \mathbf{k}), \tag{14}$$

$$\epsilon^2_{\mathbf{k}} = E^2_{\mathbf{k}} - B^2_{\mathbf{k}}, \tag{15}$$

$$\Omega(\omega, \mathbf{k}) = E_{\mathbf{k}}(\Sigma + \bar{\Sigma}) - B_{\mathbf{k}}(\Pi + \Pi^\dagger) - (\omega + \mathrm{i}\delta)(\Sigma - \bar{\Sigma}) - \Pi\Pi^\dagger + \Sigma\bar{\Sigma}, \tag{16}$$

and $\epsilon_{\mathbf{k}}$ is the spin-wave spectrum in the linear spin-wave approximation. The quantity $\Omega(\omega, \mathbf{k})$ given by equation (16) describes renormalization of the spin-wave spectrum square. We find $\Omega(\omega, \mathbf{k})$ within the first order of $1/S$ in section 4.

## 3. Classical magnon spectra

### 3.1. $H > H_c$

Let us assume first that the field is so strong that all spins lie within the plane (see figure 1). After substitution of equations (10) into equation (7) the Hamiltonian has the form $\mathcal{H} = E_0 + \sum_{i=1}^{6}\mathcal{H}_i$, where $E_0$ is the ground state energy and $\mathcal{H}_i$ denote terms containing products of $i$ operators $a$ and $a^\dagger$. $\mathcal{H}_1 = 0$ because it contains only $Q^{\rho\beta}_{\mathbf{0}}$ with $\rho \neq \beta$. For $\mathcal{H}_2$ one has equation (12), where

$$\begin{aligned} E_{\mathbf{k}} &= S(J_{\mathbf{0}} - J_{\mathbf{k}}) - \frac{S}{2}\left(Q^{xx}_{\mathbf{k}} + Q^{yy}_{\mathbf{k}} - \frac{2\omega_0\alpha}{3}\right) \\ &\quad + H - AS\left(1 - \frac{1}{2S}\right) \\ &\overset{k\ll 1}{\approx} Dk^2 - \frac{S\omega_0}{4}k\cos^2\phi_{\mathbf{k}} \\ &\quad + H - AS\left(1 - \frac{1}{2S}\right) + \frac{S\omega_0\alpha}{2}, \end{aligned} \tag{17}$$

$$\begin{aligned} B_{\mathbf{k}} &= \frac{S}{2}(Q^{yy}_{\mathbf{k}} - Q^{xx}_{\mathbf{k}}) + AS\left(1 - \frac{1}{4S}\right) \\ &\overset{k\ll 1}{\approx} -\frac{S\omega_0\alpha}{2} + \frac{S\omega_0}{4}k(1 + \sin^2\phi_{\mathbf{k}}) + AS\left(1 - \frac{1}{4S}\right), \end{aligned} \tag{18}$$

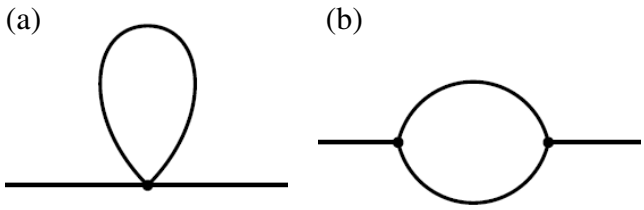


**Figure 2.** Diagrams of the first order in $1/S$ for self-energy parts. Diagram (a) stems from four-magnon terms in the Hamiltonian whereas (b) comes from three-magnon terms.

where $\phi_{\mathbf{k}}$ is the angle between $\mathbf{k}$ and the magnetization and the expressions after $\overset{k\ll 1}{\approx}$ are approximate values of the corresponding quantities at $k \ll 1$. We find for the square of the magnon spectrum from equations (15), (17) and (18) in accordance with the well-known result [6]

$$\epsilon_{\mathbf{k}}^2 \overset{k\ll 1}{\approx} \left(Dk^2 + \frac{S\omega_0}{2} k \sin^2\phi_{\mathbf{k}} + H\right) \times (D(k-k_{c0})^2 + \Lambda^{(0)}) - \frac{A}{2} B_{\mathbf{k}}, \tag{19}$$

$$\Lambda^{(0)} = H - H_c^{(0)}, \tag{20}$$

$$H_c^{(0)} = 2SA\left(1 - \frac{1}{2S}\right) - S\omega_0\alpha + Dk_{c0}^2, \tag{21}$$

where $H_c^{(0)}$ is the classical value of the saturation field and $k_{c0}$ is given by equation (6). The second term in the first brackets in equation (19) is negligible in the considered case of $A \gg \omega_0$. The last term in equation (19) is formally of the next order in $1/S$ compared to the first one. We show below that corrections from the Hartree–Fock diagram presented in figure 2(a) cancel it and lead to renormalization of the critical field $H_c^{(0)}$. We point out also that the anisotropy constant $A$ should be accompanied by the factor $1 - 1/2S$ in all expressions for observable quantities because there is no one-ion anisotropy for $S = 1/2$ [16]. It is seen that in the zeroth order in $1/S$ (the last term in equation (19) should be discarded) the second bracket in equation (19) is positive at $H \geqslant H_c^{(0)}$ and the spectrum is stable. On the other hand, at $H < H_c^{(0)}$ the instability of the spectrum arises at momentum $\mathbf{k}_{c0}$. Notice that the direction of $\mathbf{k}_{c0}$ is not fixed within the spin-wave approximation. Meanwhile we show below that there are anisotropic corrections to the spectrum of the first order in $1/S$, which fix the direction of the vector $\mathbf{k}_{c0}$ at which the instability arises, leaving, however, the equivalence between $\mathbf{k}_{c0}$ and $-\mathbf{k}_{c0}$.

### *3.2. $H < H_c$*

Simple calculation leads to the following result for the spectrum at $k \ll 1$, assuming the collinear canted spin arrangement at $H < H_c$:

$$\epsilon_{\mathbf{k}}^2 \approx \left(Dk^2 + 2SA\left(1 - \frac{1}{2S}\right)\right)(D(k-k_{c0})^2 + 2(H_c' - H)) - S^2(Q_{\mathbf{k}}^{xz})^2 \sin^2\theta, \tag{22}$$

where $k_{c0}$ and $H_c'$ are given by equations (6) and (5), respectively, $\cos\theta = H/(2SA(1 - 1/2S) - S\omega_0\alpha)$, $\theta$ is the canting angle between spins and the field, and we have discarded terms proportional to $A$ similar to the last one in equation (19) which are of the next order in $1/S$. The second bracket in equation (22) vanishes at $k = k_{c0}$ when $H = H_c'$. The last term in equation (22) gives a negligibly small correction to $H_c'$. The spectrum (22) is unstable at $H > H_c'$. This result was obtained first in [6]. It was proposed there that a noncollinear phase arises at $T = 0$ in the interval $H_c' < H < H_c$, where $H_c$ and $H_c'$ are given up to quantum $1/S$ corrections by equations (21) and (5), respectively. We show below that the energy of the collinear phase at $H = H_c'$ is higher than that of the noncollinear one and the value of the critical field $H_c'$ is smaller (if it is nonzero at all) than that given by equation (5) and derived from the spin-wave analysis.

## 4. Spectrum renormalization at $H > H_c$

Corrections to the spectrum of the first order in $1/S$ stem from the diagrams shown in figure 2. To calculate them one should take into account terms $\mathcal{H}_3$ and $\mathcal{H}_4$ in the Hamiltonian which have the form

$$\mathcal{H}_3 = \sqrt{\frac{S}{2\mathfrak{N}}} \sum_{\mathbf{k}_1+\mathbf{k}_2+\mathbf{k}_3=\mathbf{0}} Q_2^{xz} a_{-1}^\dagger (a_{-2}^\dagger + a_2) a_3, \tag{23}$$

$$\mathcal{H}_4 = \frac{1}{8\mathfrak{N}} \sum_{\mathbf{k}_1+\mathbf{k}_2+\mathbf{k}_3+\mathbf{k}_4=\mathbf{0}} ([4A + 2(J_1 + J_3 - 2J_{1+3}) - (Q_1^{zz} + Q_3^{zz} + 4Q_{1+3}^{zz})] a_{-1}^\dagger a_{-2}^\dagger a_3 a_4 + [Q_2^{xx} - Q_2^{yy} - 2A] a_{-1}^\dagger [a_2 a_3 + a_{-2}^\dagger a_{-3}^\dagger] a_4), \tag{24}$$

where we drop index $\mathbf{k}$ in equations (23) and (24).

We have found in accordance with the conclusion of [6] that the loop diagram presented in figure 2(b) is much smaller than the Hartree–Fock one shown in figure 2(a). From the Hartree–Fock diagram one obtains for the contribution to $\Omega(\omega, \mathbf{k})$

$$\Omega(\omega, \mathbf{k}) = B_{\mathbf{k}} \frac{1}{2S\mathfrak{N}} \sum_{\mathbf{q}} B_{\mathbf{q}} \tag{25a}$$

$$- \epsilon_{\mathbf{k}}^2 \frac{1}{\mathfrak{N}} \sum_{\mathbf{q}} \frac{E_{\mathbf{q}} - \epsilon_{\mathbf{q}}}{S\epsilon_{\mathbf{q}}} \tag{25b}$$

$$+ \frac{1}{\mathfrak{N}} \sum_{\mathbf{q}} \frac{1}{\epsilon_{\mathbf{q}}} (E_{\mathbf{k}} E_{\mathbf{q}} + B_{\mathbf{k}} B_{\mathbf{q}}) \times (J_{\mathbf{q}} - J_{\mathbf{k}+\mathbf{q}} + Q_{\mathbf{q}}^{zz} - Q_{\mathbf{k}+\mathbf{q}}^{zz}) \tag{25c}$$

$$+ E_{\mathbf{k}} \frac{1}{\mathfrak{N}} \sum_{\mathbf{q}} \left[ \frac{E_{\mathbf{q}} - \epsilon_{\mathbf{q}}}{\epsilon_{\mathbf{q}}} \left( \frac{H}{S} + A - \frac{3}{2} Q_{\mathbf{q}}^{zz} \right) + \frac{B_{\mathbf{q}}^2}{S\epsilon_{\mathbf{q}}} \right] \tag{25d}$$

$$+ B_{\mathbf{k}} \frac{1}{\mathfrak{N}} \sum_{\mathbf{q}} \left[ \frac{E_{\mathbf{q}} - \epsilon_{\mathbf{q}}}{2S\epsilon_{\mathbf{q}}} B_{\mathbf{q}} + \frac{B_{\mathbf{q}}}{\epsilon_{\mathbf{q}}} \left( \frac{E_{\mathbf{q}} - \epsilon_{\mathbf{q}}}{2S} + A - \frac{3}{2} Q_{\mathbf{q}}^{zz} \right) \right]. \tag{25e}$$

Term (a) in equation (25) is equal to the first order in $1/S$ to $B_{\mathbf{k}} A/2$ and it cancels the last term in equation (19). Term (25*b*) does not renormalize the bare spectrum in the first order in $1/S$. Term (25*c*) gives rise to the anisotropic corrections to the spectrum.

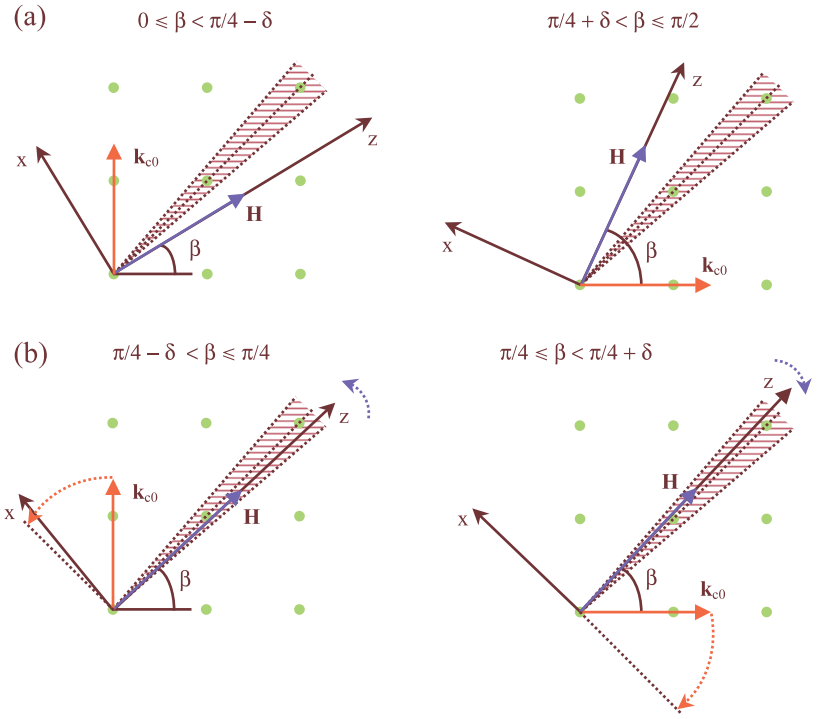


**Figure 3.** It is assumed in this paper that the field **H** lies within the plane of the lattice and is directed by an angle $\beta$ to the square edge. This figure shows the direction of the vector $\mathbf{k}_{c0}$ at which instability of the classical spin-wave spectrum arises at $H < H_c$. Domains in the stripe phase are elongated, perpendicularly to $\mathbf{k}_{c0}$. Part (a) shows the case when $\beta$ lies outside the narrow interval $(\pi/4-\delta, \pi/4+\delta)$ (cross-hatched area in the figure), where $\delta \ll 1$ is given by equation (30). Part (b) illustrates the rotation of $\mathbf{k}_{c0}$ when the field rotates inside the interval $(\pi/4-\delta, \pi/4+\delta)$. The direction of the corresponding rotations is indicated by dashed arrows. We have $\mathbf{k}_{c0} \perp \mathbf{H}$ when $\beta = \pi/4$. Notice that $\mathbf{k}_{c0}$ and $-\mathbf{k}_{c0}$ are equivalent.

It is convenient to use evident relations $E_{\mathbf{k}} = (E_{\mathbf{k}} + B_{\mathbf{k}})/2 + (E_{\mathbf{k}} - B_{\mathbf{k}})/2$ and $B_{\mathbf{k}} = (E_{\mathbf{k}} + B_{\mathbf{k}})/2 - (E_{\mathbf{k}} - B_{\mathbf{k}})/2$ to extract combinations proportional to $E_{\mathbf{k}} - B_{\mathbf{k}}$ and $E_{\mathbf{k}} + B_{\mathbf{k}}$ from terms (c)–(e) of equation (25). Terms proportional to $E_{\mathbf{k}} - B_{\mathbf{k}}$ and $E_{\mathbf{k}} + B_{\mathbf{k}}$ renormalize the first and the second brackets, respectively, in equation (19). As we are interested in the phase transition to the noncollinear phase, we focus on renormalization of the second bracket in equation (19) and consider only terms proportional to $E_{\mathbf{k}} + B_{\mathbf{k}}$.

We assume for definiteness in the particular calculations below that $J \gg A \gg \omega_0$. As a result of simple but tedious calculations one has from equation (25) in the leading order of $\omega_0/J$ and $A/J$ for the important (for us) terms

$$\Omega(\omega, \mathbf{k}) \sim \frac{A}{2} B_{\mathbf{k}} + (E_{\mathbf{k}} + B_{\mathbf{k}}) \times \left( k^2 \omega_0 [X \cos(2\phi_{\mathbf{k}} + 2\beta) \cos 2\beta + Y \cos^2 \phi_{\mathbf{k}}] + \frac{A}{\mathfrak{N}} \sum_{\mathbf{q}} \frac{B_{\mathbf{q}}}{\epsilon_{\mathbf{q}}} \right), \tag{26}$$

$$X = \frac{D}{16 S \omega_0 \mathfrak{N}} \sum_{\mathbf{q}} \frac{Q^{xx}_{\mathbf{q}} - Q^{zz}_{\mathbf{q}}}{J_0 - J_{\mathbf{q}}} (\cos q_x - \cos q_z), \tag{27}$$

$$Y = \frac{3}{2^7 \pi} \sqrt{\frac{2AS}{D}} \ln \left( 32 \frac{ASD}{(S\omega_0)^2} \right), \tag{28}$$

where $\beta$ is the angle between the magnetic field and an edge of the square (see figure 3). The constant $X$ should be calculated numerically because summation over large momenta is important in equation (27) and one cannot use equations (8) and (9) for the dipolar tensor components. This calculation can be carried out using the dipolar sums computation technique (see, for example, [17] and references therein) with the result $X \approx 0.0087$ for exchange coupling between only nearest neighbor spins on the simple square lattice.

Terms in equation (26) proportional to $X$ and $Y$ stem from parts of the term (25*c*) in equation (25) proportional to $J_{\mathbf{q}} - J_{\mathbf{k}+\mathbf{q}}$ and $Q^{zz}_{\mathbf{q}} - Q^{zz}_{\mathbf{k}+\mathbf{q}}$, respectively. They make a negligibly small correction to the constant $D$ in the second bracket in equation (19). Meanwhile they are very important for our considerations because they fix the direction of the momentum at which the spectral instability arises: $\mathbf{k}_{c0}$ is directed so that this term is minimal at $\phi_{\mathbf{k}} = \phi_{\mathbf{k}_{c0}}$. Notice that anisotropic terms are invariant according to the replacement $\phi_{\mathbf{k}} \mapsto \phi_{\mathbf{k}} \pm \pi$. Then $\mathbf{k}_{c0}$ and $-\mathbf{k}_{c0}$ are equivalent. One obtains after simple calculations that the anisotropic part in equation (26) has a minimum at $\phi_{\mathbf{k}_{c0}}$ given by

$$\tan 2\phi_{\mathbf{k}_{c0}} = -\frac{\sin 4\beta}{Y/X + 2\cos^2 2\beta}, \tag{29}$$

where the solution should be taken with $\cos 2\phi_{\mathbf{k}_{c0}} < 0$. The term $Y/X$ plays a part in equation (29) only when $\beta \approx \pi/4$, because $X \gg Y$. Simple calculation shows that the first and the second terms in the denominator in equation (29) are equal

at $\beta = \pi/4 \pm \delta$, where

$$\delta = \sqrt{\frac{Y}{8X}} \sim \left(\frac{AS}{D}\right)^{1/4} \ll 1. \tag{30}$$

Then, when $\beta$ lies outside the narrow interval $(\pi/4-\delta, \pi/4+\delta)$ the term with $Y$ can be discarded in equation (29) and one has for $\phi_{\mathbf{k}_{c0}}$

$$\phi_{\mathbf{k}_{c0}} = \begin{cases} \pi/2 - \beta, & \text{if } \beta \in [0, \pi/4 - \delta), \\ -\beta, & \text{if } \beta \in (\pi/4 + \delta, \pi/2]. \end{cases} \tag{31}$$

Equation (31) signifies that $\mathbf{k}_{c0}$ does not rotate with the field and is directed along the square edge as shown in figure 3(a). On the other hand, the term with $Y$ comes into play when $\beta$ lies in the interval $(\pi/4 - \delta, \pi/4 + \delta)$ and $\mathbf{k}_{c0}$ rotates in the same direction as the field $\mathbf{H}$, so that $\mathbf{k}_{c0}$ turns out to be perpendicular to $\mathbf{H}$ when $\beta = \pi/4$ (see figure 3(b)).

The last term in equation (26) leads to quantum renormalization of the critical field $H_c$ which has the form

$$H_c = H_c^{(0)} - \frac{A^2 S}{4\pi D} \ln\left(\frac{D}{2AS}\right) \tag{32}$$

when $\ln(D/AS) \gg 1$, where $H_c^{(0)}$ is given by equation (21). It is seen from equation (32) that quantum fluctuations reduce the value of the saturation field. As a result we have for the spin-wave spectrum at $k \ll 1$

$$\epsilon_{\mathbf{k}}^2 \approx (Dk^2 + H)(D(k - k_{c0})^2 + \Lambda + \delta(\phi_{\mathbf{k}})), \tag{33}$$

$$\Lambda = H - H_c, \tag{34}$$

where $H_c$ is given by equation (32) and $\delta(\phi_{\mathbf{k}})$ stands for the small anisotropic terms discussed above.

## 5. The noncollinear phase

We discuss in this section properties of the noncollinear phase. Spin arrangement is considered at $H \approx H_c$ and $H < H_c$ in sections 5.1 and 5.2, respectively. The spin-wave spectrum is discussed in section 5.3.

### *5.1. Transition from the collinear phase to the noncollinear one at $H = H_c$*

It was shown in the previous section that the spectrum (33) of the collinear phase becomes unstable when $\Lambda < 0$, i.e. when $H < H_c$. The instability occurs at a momentum $\mathbf{k}_{c0}$, the absolute value of which is given by equation (6) and the direction is determined by small $1/S$-corrections. This instability signifies a transition to a noncollinear phase. We discuss now the spin arrangement in this phase using the approach of Bose–Einstein condensation of magnons [8].

There are two equivalent minima in the bare spectrum (33) at momenta $\pm\mathbf{k}_{c0}$. The instability of the spectrum at $\mathbf{k} = \pm\mathbf{k}_{c0}$ at an $H$ slightly smaller than $H_c$, meaning a 'condensation' of magnons at states with these momenta. It is shown below that at $H < H_c$ the energy can be lowered by varying the value of the momentum $\mathbf{k}_c \parallel \mathbf{k}_{c0}$ at which the condensation takes place. Thus, $k_c$ depends on $H$ so that $k_c = k_{c0}$ at $H = H_c$ and $k_c < k_{c0}$ at $H < H_c$. Then we imply below that $k_c \neq k_{c0}$.

At $H < H_c$ one should replace the operator $a_{\pm\mathbf{k}_c}$ and $a^\dagger_{\pm\mathbf{k}_c}$ as follows

$$\begin{aligned} a_{\pm\mathbf{k}_c} &\mapsto a_{\pm\mathbf{k}_c} + \mathrm{e}^{\mathrm{i}\varphi_1}\sqrt{\mathfrak{N}\rho_{\mathbf{k}_c}}, \\ a^\dagger_{\pm\mathbf{k}_c} &\mapsto a^\dagger_{\pm\mathbf{k}_c} + \mathrm{e}^{-\mathrm{i}\varphi_1}\sqrt{\mathfrak{N}\rho_{\mathbf{k}_c}}, \end{aligned} \tag{35}$$

where $\rho_{\mathbf{k}_c}$ is the density of condensed particles and $\varphi_1$ is a phase constant which should be found from the demand that linear terms disappear in the Hamiltonian arising after transformation (35) (see, e.g. [18]). Taking into account the equivalence of minima at $+\mathbf{k}_c$ and $-\mathbf{k}_c$ we assume in equation (35) that $\rho_{\mathbf{k}_c} = \rho_{-\mathbf{k}_c}$ and similar equalities are implied below for harmonics of $\mathbf{k}_c$. One has from equations (12) and (24) for the term in the Hamiltonian linear in $a^\dagger_{\mathbf{k}_c}$

$$\begin{aligned} &\sqrt{\mathfrak{N}\rho_{\mathbf{k}_c}}(\mathrm{e}^{\mathrm{i}\varphi_1} E_{\mathbf{k}_c} + \mathrm{e}^{-\mathrm{i}\varphi_1} B_{\mathbf{k}_c} \\ &\quad + 3A\rho_{\mathbf{k}_c}(\mathrm{e}^{\mathrm{i}\varphi_1} - \tfrac{1}{4}\mathrm{e}^{\mathrm{i}3\varphi_1} - \tfrac{3}{4}\mathrm{e}^{-\mathrm{i}\varphi_1}))a^\dagger_{\mathbf{k}_c}. \end{aligned} \tag{36}$$

We obtain the term linear in $a_{\mathbf{k}_c}$ by conjugating equation (36). In order for expression (36) to be equal to zero at nonzero positive $\rho_{\mathbf{k}_c}$, $\varphi_1$ should be equal to $\pm\pi/2$. We choose a plus sign below, and one obtains that equation (36) is equal to zero when

$$\begin{aligned} \varphi_1 &= \frac{\pi}{2}, \\ \rho_{\mathbf{k}_c} &= -\frac{E_{\mathbf{k}_c} - B_{\mathbf{k}_c}}{6A} = -\frac{D(k_c - k_{c0})^2 + \Lambda}{6A}. \end{aligned} \tag{37}$$

It is seen that a positive solution for $\rho_{\mathbf{k}_c}$ exists only if $\Lambda < 0$, i.e. at $H < H_c$. Notice that the solution (37) also corresponds to the result of minimization with respect to $\varphi_1$ and $\rho_{\mathbf{k}_c}$ of the correction to the energy arising after transformation (35) and given by

$$\frac{\mathcal{E}_1}{\mathfrak{N}} = 2\rho_{\mathbf{k}_c}(E_{\mathbf{k}_c} + B_{\mathbf{k}_c}\cos 2\varphi_1) + 3A\rho_{\mathbf{k}_c}^2(1 - \cos 2\varphi_1). \tag{38}$$

Minimization of $\mathcal{E}_1$ with respect to $k_c$ gives $k_c = k_{c0}$. The deviation of $k_c$ from $k_{c0}$ arises after taking into account condensation of magnons at states characterized by harmonics of $\mathbf{k}_c$.

It is seen from equation (24) that transformation (35) also leads to terms in the Hamiltonian linear in $a_{\pm 3\mathbf{k}_c}$ and $a^\dagger_{\pm 3\mathbf{k}_c}$. In order to cancel these terms one has to perform the following transformation of $a_{\pm 3\mathbf{k}_c}$ and $a^\dagger_{\pm 3\mathbf{k}_c}$ similar to (35)

$$\begin{aligned} a_{\pm 3\mathbf{k}_c} &\mapsto a_{\pm 3\mathbf{k}_c} + \mathrm{e}^{\mathrm{i}\varphi_3}\sqrt{\mathfrak{N}\rho_{3\mathbf{k}_c}}, \\ a^\dagger_{\pm 3\mathbf{k}_c} &\mapsto a^\dagger_{\pm 3\mathbf{k}_c} + \mathrm{e}^{-\mathrm{i}\varphi_3}\sqrt{\mathfrak{N}\rho_{3\mathbf{k}_c}}. \end{aligned} \tag{39}$$

As a result the term in the Hamiltonian linear in $a^\dagger_{3\mathbf{k}_c}$ arising after transformation (39) has the form

$$\begin{aligned} &\sqrt{\mathfrak{N}}\big(\sqrt{\rho_{3\mathbf{k}_c}}\left(\mathrm{e}^{\mathrm{i}\varphi_3} E_{3\mathbf{k}_c} + \mathrm{e}^{-\mathrm{i}\varphi_3} B_{3\mathbf{k}_c}\right) + 2\mathrm{i}A\rho_{\mathbf{k}_c}^{3/2} \\ &\quad + A\rho_{\mathbf{k}_c}\sqrt{\rho_{3\mathbf{k}_c}}\left(7\mathrm{e}^{\mathrm{i}\varphi_3} - 5\mathrm{e}^{-\mathrm{i}\varphi_3}\right)\big)a^\dagger_{3\mathbf{k}_c}. \end{aligned} \tag{40}$$

This is equal to zero if

$$\begin{aligned} \varphi_3 &= -\frac{\pi}{2}, \\ \sqrt{\rho_{3\mathbf{k}_c}} &= -\sqrt{\rho_{\mathbf{k}_c}}\frac{1}{3}\frac{D(k_c - k_{c0})^2 + \Lambda}{D(3k_c - k_{c0})^2 - 2D(k_c - k_{c0})^2 - \Lambda}. \end{aligned} \tag{41}$$

Solution (41) also corresponds to the result of minimization with respect to $\varphi_3$ and $\rho_{3\mathbf{k}_c}$ of the correction to the energy arising after transformation (39) that has the form

$$\frac{\mathcal{E}_3}{\mathfrak{N}} = 2\rho_{3\mathbf{k}_c}(E_{3\mathbf{k}_c} + B_{3\mathbf{k}_c}\cos 2\varphi_3) + 8A\rho_{\mathbf{k}_c}^{3/2}\sqrt{\rho_{3\mathbf{k}_c}}\sin\varphi_1\sin\varphi_3 + 2A(7-5\cos 2\varphi_3)\rho_{\mathbf{k}_c}\rho_{3\mathbf{k}_c}. \quad (42)$$

Condensation of magnons at states characterized by harmonics of $\mathbf{k}_c$ makes it possible to lower the energy further by varying the absolute value of $\mathbf{k}_c$ at any given $H$. To show this, let us consider the first terms in equations (38) and (42) which are the only terms depending on $k_c$ in these expressions. Their explicit forms are $2\rho_{\mathbf{k}_c}(D(k_c-k_{c0})^2+\Lambda)$ and $2\rho_{3\mathbf{k}_c}(D(3k_c-k_{c0})^2+\Lambda)$, respectively. It seen that at any fixed $\rho_{\mathbf{k}_c}$ and $\rho_{3\mathbf{k}_c}$ a small deviation of $k_c$ from $k_{c0}$ (to be precise, a small decrease) raises $\mathcal{E}_1$ and lowers $\mathcal{E}_3$. The total energy reduces in this case because $\mathcal{E}_1$ rises quadratically with $(k_c - k_{c0})$ and $\mathcal{E}_3$ reduces linearly with $(k_c - k_{c0})$. As a result minimization of the total energy correction $\mathcal{E}_1 + \mathcal{E}_3$ with respect to $k_c$ gives in the leading order in $\Lambda/Dk_{c0}^2$

$$k_c = k_{c0}\left(1 - \frac{1}{24}\left(\frac{\Lambda}{Dk_{c0}^2}\right)^2\right). \quad (43)$$

Notice also that $\mathbf{k}_c$ should be parallel to $\mathbf{k}_{c0}$ because the absolute value of negative anisotropic corrections to $D$ discussed in section 4 has a maximum when $\mathbf{k}_c \| \mathbf{k}_{c0}$. It is seen from equations (41) and (43) that $\rho_{3\mathbf{k}_c} \ll \rho_{\mathbf{k}_c}$ if $H \approx H_c$. We use this fact in equations (40) and (42) discarding terms of powers in $\rho_{3\mathbf{k}_c}$ higher than 1/2 and 1, respectively, and omitting terms with higher harmonics in equations (36), (38), (40) and (42).

It is easy to show that the phase factor of the $(2n+1)$ th harmonic of $\mathbf{k}_c$ should be equal to $\pi/2$ or $-\pi/2$ in order that the linear terms can vanish in the Hamiltonian. One has to take into account the fact that terms in the Hamiltonian linear in $a_{(2n+1)\mathbf{k}_c}$ and $a^\dagger_{(2n+1)\mathbf{k}_c}$ stem from $\mathcal{H}_q$ with even $q$ and that $E_{(2n+1)\mathbf{k}_c} \approx B_{(2n+1)\mathbf{k}_c} \approx SA$ if $n$ is not very large. Closer examination gives

$$\varphi_{2n+1} = (-1)^n\frac{\pi}{2}. \quad (44)$$

For instance, it is seen from equation (42) that $\varphi_1$ and $\varphi_3$ should have different signs to minimize the second term. The validity of equation (44) for higher harmonics is not so evident for large enough $|\Lambda|$, at which densities of condensed particles at states characterized by neighboring higher harmonics differ several times only. Meanwhile, particular numerical calculations show the validity of equation (44) in this case too.

Terms in the Hamiltonian with an odd number of operators $a$ and $a^\dagger$ which are proportional to Fourier components of the non-diagonal parts of the dipolar tensor $Q^{xz}$ (see, for example, equation (23)) lead to condensation of magnons at states characterized by even harmonics of $\mathbf{k}_c$. It is easy to show that phase constants $\varphi_{2n}$ should be equal to zero modulo $\pi$ in corresponding transformations similar to (35) and (39). The density of condensed particles is very small at states characterized by even harmonics of $\mathbf{k}_c$. For instance, $\rho_{2\mathbf{k}_c} \propto \rho_{\mathbf{k}_c}^2(Q^{xz}_{2\mathbf{k}_c}/A)^2 \ll \rho_{\mathbf{k}_c}$. Notice that $\rho_{2n\mathbf{k}_c} = 0$ when $\mathbf{k}_c \perp \mathbf{H}$ because $Q^{xz}_{2n\mathbf{k}_c} = 0$ in this case. The density of condensed particles in the state with zero momentum $\rho_\mathbf{0}$ is equal to zero at any $\mathbf{k}_c$ direction because $Q^{xz}_\mathbf{0} = 0$.

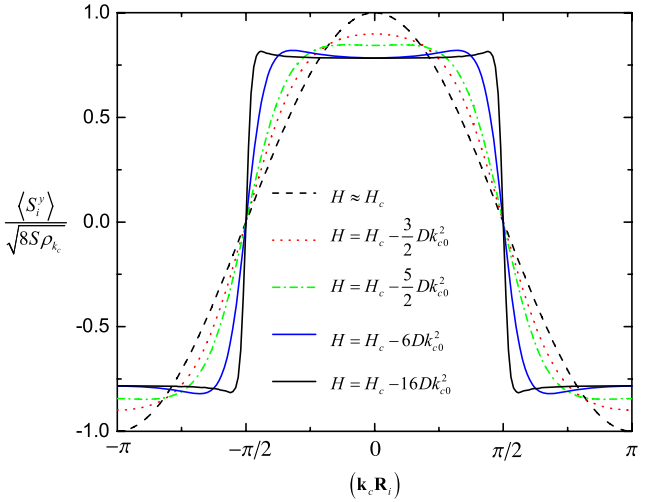


**Figure 4.** The value $\langle S_i^y\rangle/\sqrt{8S\rho_{\mathbf{k}_c}}$ given by equation (45) is shown in the noncollinear phase (i.e. at $H < H_c$) to demonstrate the field evolution of the domain pattern profile formed by off-plane spins components (see figure 1). It is seen that the profile is sinusoidal at $H \approx H_c$ and evolves with decreasing field into a meander-like and then into a step-like form. Notice that the period of the stripe structure increases with decreasing field as illustrated in figure 5.

One can find the spin ordering in the noncollinear phase at $H \approx H_c$ using equations (37), (41) and (43). We obtain mean values of the transverse spin components $\langle S^x_\mathbf{k}\rangle \approx \sqrt{2S}\langle a_\mathbf{k} + a^\dagger_{-\mathbf{k}}\rangle/2$ and $\langle S^y_\mathbf{k}\rangle \approx \sqrt{2S}\langle a_\mathbf{k} - a^\dagger_{-\mathbf{k}}\rangle/2\mathrm{i}$ using the fact that $\langle a_{n\mathbf{k}_c}\rangle = \mathrm{e}^{\mathrm{i}\varphi_n}\sqrt{\mathfrak{N}\rho_{n\mathbf{k}_c}}$. Only even and odd harmonics contribute to $\langle S_i^x\rangle$ and $\langle S_i^y\rangle$, respectively, because $\varphi_{2n+1} = \pm\pi/2$ and $\varphi_{2n} = 0 \bmod \pi$ and we have

$$\langle S_i^y\rangle = \sqrt{8S\rho_{\mathbf{k}_c}}\left(\cos(\mathbf{k}_c\mathbf{R}_i) + \sum_{n=1}^{\infty}(-1)^n\sqrt{\frac{\rho_{(2n+1)\mathbf{k}_c}}{\rho_{\mathbf{k}_c}}}\cos((2n+1)\mathbf{k}_c\mathbf{R}_i)\right). \quad (45)$$

Due to the very low densities of condensed particles at states with even harmonics we do not discuss $\langle S_i^x\rangle$ here. As $\rho_{(2n+1)\mathbf{k}_c} \ll \rho_{\mathbf{k}_c}$ when $H \approx H_c$, only the first few terms come into play in equation (45) at such $H$. We plot the value $\langle S_i^y\rangle/\sqrt{8S\rho_{\mathbf{k}_c}}$ in figure 4 for $H \approx H_c$ and $H = H_c - 1.5Dk_{c0}^2$ using equations (37), (41), (43) and (45). It is seen that $\langle S_i^y\rangle$ has a sinusoidal profile at $H \approx H_c$, as shown in figure 1, that is slightly distorted at smaller fields due to the higher harmonics in equation (45). Higher harmonics in equation (45) become important at $H < H_c - 1.5Dk_{c0}^2$ when they change considerably the profile of $\langle S_i^y\rangle$ (i.e. the domain pattern profile) which we discuss in section 5.2.

Let us compare energies of the stripe phase and the collinear canted phase at $H < H_c$. The last one can be found performing the transformation for operators $a_\mathbf{0}$ and $a^\dagger_\mathbf{0}$ similar to (35) and (39) and minimizing the corresponding expression

for the energy correction. The result is

$$\frac{\mathcal{E}_0}{\mathfrak{N}} = -\frac{(E_\mathbf{0} - B_\mathbf{0})^2}{4A} = -\frac{(Dk_{c0}^2 - |\Lambda|)^2}{4A}. \qquad (46)$$

This expression gives the value of the energy correction as higher than that of the stripe phase. For example, corresponding values for $H = H_c'$ are $-0.179\Lambda^2/A$ and $-0.063\Lambda^2/A$ for the stripe and the canted collinear phase, respectively, where $H_c'$ given by equation (5) is the field below which the classical spin-wave spectrum of the canted phase is stable. The difference between energies of the collinear canted phase and the stripe phase decreases as the field reduces.

### 5.2. $H < H_c$

We demonstrate in the appendix that the expression for the energy of the noncollinear phase is much more complicated at $H < H_c$ because one has to take into account corrections to the energy containing $\rho_{(2n+1)\mathbf{k}_c}$ with $n > 1$ for accurate finding of the stripe profile and $k_c$. The corresponding values of $\rho_{(2n+1)\mathbf{k}_c}$ and $k_c$ have to be found by numerical minimization of the energy. The number of harmonics of $\mathbf{k}_c$ to be taken into account in particular calculations rises as the field decreases. For example, we find that one can use only five harmonics for $H = H_c - 2.5Dk_{c0}^2$ whereas their number should be increased to 51 for $H = H_c - 16Dk_{c0}^2$. This circumstance leads to a restriction on the field interval which can be considered practically. The smallest field value we have managed to reach is $H = H_c - 16Dk_{c0}^2$.

We plot $\langle S_i^y\rangle/\sqrt{8S\rho_{\mathbf{k}_c}}$ in figure 4 for some $H$ values using equation (45) and the results of numerical calculation of $\rho_{(2n+1)\mathbf{k}_c}$. We used equations (37), (41) and (43) for $H = H_c - 1.5Dk_{c0}^2$ and equations (A.6) for $H = H_c - 2.5Dk_{c0}^2$. It is seen that the sinusoidal profile evolves with decreasing field into a meander-like and then into a step-like form. Then, the domain wall density decreases from unity to a value much smaller than unity with decreasing field.

The dependence of $k_c$ on $H$ is illustrated in figure 5. Notice that the period of the stripe structure given by $2\pi/k_c$ rises very fast as the field decreases. This finding is in qualitative agreement with the results of [5], where a very large period of the stripe pattern was found at $H = 0$ when $A \gg \omega_0$.

### 5.3. Spin-wave spectrum in the noncollinear phase

There are two types of corrections to the bilinear part of the Hamiltonian (12) arising after transformation (35). The first one leads to the following simple renormalization of $E_\mathbf{k}$ and $B_\mathbf{k}$:

$$E_\mathbf{k} \mapsto E_\mathbf{k} + 7A\rho_{\mathbf{k}_c}, \qquad B_\mathbf{k} \mapsto B_\mathbf{k} - 5A\rho_{\mathbf{k}_c}. \qquad (47)$$

This renormalization gives rise to an additional term equal to $2|\Lambda|$ in the second bracket in equation (33) and the spectrum takes the form

$$\epsilon_\mathbf{k}^2 \approx (Dk^2 + H)(D(k - k_c)^2 + |\Lambda|). \qquad (48)$$

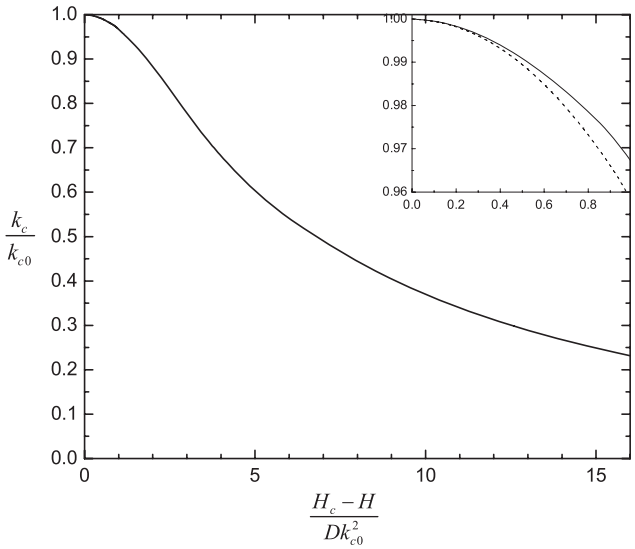


**Figure 5.** Dependence of the absolute value of the momentum $\mathbf{k}_c$, describing the stripe structure, on the magnetic field found by numerical energy minimization taking into account 51 harmonics of $\mathbf{k}_c$. The inset shows the neighborhood of point $H = H_c$, where the dependence of $k_c$ on $H$ is described by the approximate analytical expression (43) (dashed line).

Higher harmonics contribute to renormalization of $E_\mathbf{k}$ and $B_\mathbf{k}$ as well but their effect is small at $|\Lambda| < Dk_{c0}^2$ because corresponding densities are much smaller than $\rho_{\mathbf{k}_c}$.

Another sort of correction to the bilinear part of the Hamiltonian includes the so-called umklapp interaction having the form

$$A\rho_{\mathbf{k}_c}\sum_\mathbf{k}[\tfrac{7}{2}a_\mathbf{k}^\dagger a_{\mathbf{k}\pm2\mathbf{k}_c} - \tfrac{5}{4}\left(a_\mathbf{k}a_{-\mathbf{k}\pm2\mathbf{k}_c} + a_\mathbf{k}^\dagger a_{-\mathbf{k}\pm2\mathbf{k}_c}^\dagger\right)]. \qquad (49)$$

There are also terms given by equation (49) with $2n\mathbf{k}_c$ and $\rho_{n\mathbf{k}_c}$ instead of $2\mathbf{k}_c$ and $\rho_{\mathbf{k}_c}$ with $n > 1$ which can be neglected at $|\Lambda| < Dk_{c0}^2$. The umklapp interaction makes the spin-wave spectrum analysis much more complicated (see, for example, [19], for some detail). It can also be shown that corrections to the spectrum square from umklapp terms (49) are negligible for momenta with absolute values that are not very close to $k_c$: $D(k - k_c)^2 \gtrsim |\Lambda|$. Then the spectrum is given by equation (48) in this case. Carrying out a much more complicated analysis for $k \approx k_c$ is outside the scope of the present work.

## 6. Conclusion

In conclusion, we discuss a 2D Heisenberg ferromagnet with dipolar forces and out-of-plane easy-axis one-ion anisotropy in an in-plane magnetic field described by the Hamiltonian (1). We consider the classical spin-wave spectrum assuming a collinear spin arrangement and find in accordance with previous results [6] that the spectrum is unstable in a range of fields $H_c' < H < H_c$, where $H_c$ is the saturation field given by equation (32) and $H_c'$ is given by equation (5). The instability arises at an incommensurate momentum $\mathbf{k}_{c0}$, the direction of which is not fixed in the linear spin-wave approximation and

the absolute value of which is given by equation (6). Thus, we conclude, following [6], that the collinear spin arrangement is unstable at $H < H_c$ with respect to stripe domain formation with a large period (see figure 1).

To discuss the properties of the noncollinear phase we first consider $1/S$ corrections to the spectrum of the collinear phase at $H > H_c$ and find that they fix the direction of $\mathbf{k}_{c0}$ so that it depends on the field direction as shown in figure 3. We discuss the noncollinear phase using the technique of Bose–Einstein condensation of magnons suggested in [8]. The appearance of the stripe spin arrangement corresponds in this technique to a 'condensation' of magnons at $H < H_c$ at states characterized by a momentum $\mathbf{k}_c \| \mathbf{k}_{c0}$ and its harmonics (i.e. $n\mathbf{k}_c$, where $n$ is integer). It is the unusual result of the present analysis that the vector $\mathbf{k}_c$ varies with the field (remaining parallel to $\mathbf{k}_{c0}$) so that $k_c = k_{c0}$ at $H = H_c$ and $k_c < k_{c0}$ at $H < H_c$. This behavior originates in the condensation of magnons at states characterized by harmonics of $\mathbf{k}_c$.

We demonstrate that the energy of the stripe phase is lower than the energy of any collinear spin arrangement at $H < H_c$ but the difference between these energies decreases as the field reduces. We have not found any sign of transition to a collinear phase at $H \lesssim H_c$. Then, $H_c'$ given by equation (5) is overestimated in the previous work [6] in which it was obtained from the condition of the spin-wave spectrum stability in the collinear canted phase. It should be noted that our finding is in qualitative agreement with the results of [5], where it was shown, in particular, that at $H = 0$ the difference between energies of the stripe pattern and the collinear phase is very small in the limiting case of $A \gg \omega_0$ discussed in the present paper.

Expression of the values of spin components perpendicular to the film forming the domain pattern is given by equation (45). Coefficients $\rho_{n\mathbf{k}_c}$ and the value of $k_c$ are obtained by numerical minimization of the ground state energy. The transformation of the domain pattern upon the variation of the field is shown in figure 4. It is seen that the domain pattern has a sinusoid profile at $H \approx H_c$ that transforms to a step-like profile with decreasing field so that the domain wall density decreases from unity to a value much smaller than unity. The dependence of $k_c$ on the field is shown in figure 5. It is seen that the period of the stripe pattern ($2\pi/k_c$) rises very quickly as the field decreases. This finding is also in qualitative agreement with results of [5], where it was shown that at $H = 0$ the period of the stripe structure is very large at $A \gg \omega_0$.

We find that the spin-wave spectrum in the noncollinear phase is given by equation (48) for momenta $D(k-k_c)^2 \gtrsim |\Lambda|$ if $|\Lambda| < Dk_{c0}^2$.

## Acknowledgments

This work was supported by Russian Science Support Foundation, President of Russian Federation (grant MK-1056.2008.2), RFBR grants 09-02-00229 and 07-02-01318, and Russian Programs 'Quantum Macrophysics', 'Strongly correlated electrons in semiconductors, metals, superconductors and magnetic materials' and 'Neutron Research of Solids'.

## Appendix. Energy of the noncollinear phase

We present in this appendix some details about the noncollinear phase energy calculation that was used in finding the value of $k_c$ drawn in figure 5 and the domain pattern profile presented in figure 4. It is convenient to express the correction to the energy arising after transformations (35) and (39) (and similar ones for higher harmonics of $\mathbf{k}_c$) in the following form:

$$\mathcal{E} = \sum_{n=0}^{\infty} \mathcal{E}_{2n+1}, \tag{A.1}$$

where $\mathcal{E}_{2n+1}$ contains all terms depending on $\rho_{(2n+1)\mathbf{k}_c}$ and not depending on $\rho_{(2i+1)\mathbf{k}_c}$ with $i > n$. In particular, one has for the first three terms in equation (A.1)

$$\mathcal{E}_1 = 2\rho_{\mathbf{k}_c}(D(k_c - k_{c0})^2 - |\Lambda|) + 6A\rho_{\mathbf{k}_c}^2, \tag{A.2}$$

$$\mathcal{E}_3 = -8A\rho_{\mathbf{k}_c}^{3/2}\sqrt{\rho_{3\mathbf{k}_c}} + 24A\rho_{\mathbf{k}_c}\rho_{3\mathbf{k}_c} + 6A\rho_{3\mathbf{k}_c}^2 + 2\rho_{3\mathbf{k}_c}(D(3k_c - k_{c0})^2 - |\Lambda|), \tag{A.3}$$

$$\mathcal{E}_5 = -24A\rho_{\mathbf{k}_c}\sqrt{\rho_{3\mathbf{k}_c}\rho_{5\mathbf{k}_c}} + 24A\rho_{3\mathbf{k}_c}\sqrt{\rho_{\mathbf{k}_c}\rho_{5\mathbf{k}_c}} + 24A(\rho_{\mathbf{k}_c} + \rho_{3\mathbf{k}_c})\rho_{5\mathbf{k}_c} + 6A\rho_{5\mathbf{k}_c}^2 + 2\rho_{5\mathbf{k}_c}(D(5k_c - k_{c0})^2 - |\Lambda|), \tag{A.4}$$

where we take into account equation (44) for phase factors $\varphi_{2n+1}$. We can restrict ourselves to some first terms in equation (A.1) to perform the numerical minimization of $\mathcal{E}$ because the value of $\rho_{(2n+1)\mathbf{k}_c}$ decreases as $n$ rises. Meantime, the number of terms to be taken into account in equation (A.1) increases as the field decreases. For example, we find that one can use only terms (A.2)–(A.4) for $H = H_c - 2.5Dk_{c0}^2$. The corresponding values of $k_c$ and densities are given by

$$k_c \approx 0.832k_{c0}, \tag{A.5}$$

$$\rho_{\mathbf{k}_c} \approx 1.13\frac{|\Lambda|}{6A}, \qquad \sqrt{\frac{\rho_{3\mathbf{k}_c}}{\rho_{\mathbf{k}_c}}} \approx 0.183, \qquad \sqrt{\frac{\rho_{5\mathbf{k}_c}}{\rho_{\mathbf{k}_c}}} \approx 0.0325, \qquad \sqrt{\frac{\rho_{7\mathbf{k}_c}}{\rho_{\mathbf{k}_c}}} \approx 0.0057, \tag{A.6}$$

which, in particular, have been put into equation (45) to plot $\langle S_i^y \rangle / \sqrt{8S\rho_{\mathbf{k}_c}}$ in figure 4. We have obtained that one has to take into account 26 terms in equation (A.1) for $H = H_c - 16Dk_{c0}^2$.

## References

[1] De'Bell K, MacIsaac A B and Whitehead J P 2000 *Rev. Mod. Phys.* **72** 225
[2] Jensen P J and Bennemann K H 2007 *Surf. Sci. Rep.* **61** 129
[3] Pappas D P, Kämper K-P and Hopster H 1990 *Phys. Rev. Lett.* **64** 3179
[4] Allenspach R, Stampanoni M and Bischof A 1990 *Phys. Rev. Lett.* **65** 3344
[5] Yafet Y and Gyorgy E M 1988 *Phys. Rev.* B **38** 9145
[6] Erickson R P and Mills D L 1992 *Phys. Rev.* B **46** 861
[7] Gubbiotti G, Carlotti G, Pini M G, Politi P, Rettori A, Vavassori P, Ciria M and O'Handley R C 2002 *Phys. Rev.* B **65** 214420
[8] Batyev E G and Braginskii L S 1984 *Sov. Phys.—JETP* **60** 781
[9] Syromyatnikov A V 2007 *Phys. Rev.* B **75** 134421
[10] Maleev S V 1976 *Sov. Phys.—JETP* **43** 1240

[11] Dantziger M, Glinsmann B, Scheffler S, Zimmermann B and Jensen P J 2002 *Phys. Rev.* B **66** 094416
[12] Syromyatnikov A V 2008 *Phys. Rev.* B **77** 014435
[13] Syromyatnikov A V 2006 *Phys. Rev.* B **74** 014435
[14] Akhiezer A I, Bar'yakhtar V G and Peletminskii S V 1968 *Spin Waves* (Amsterdam: North-Holland)
[15] Holstein T and Primakoff H 1940 *Phys. Rev.* **58** 1098
[16] Chubukov A V 1985 *JETP* **62** 762
[17] Cohen M H and Keffer F 1955 *Phys. Rev.* **99** 1128
[18] Popov V N 1987 *Functional Integrals and Collective Excitations* (Cambridge: Cambridge University Press)
[19] Maleyev S V 2006 *Phys. Rev.* B **73** 174402